

Selective epitaxial growth of submicron complex oxide structures by amorphous SrTiO₃

P. Morales,^{a)} M. DiCiano, and J. Y. T. Wei

Department of Physics, University of Toronto, 60 St. George Street, Toronto, Ontario M5S1A7, Canada

(Received 21 February 2005; accepted 24 March 2005; published online 5 May 2005)

A chemical-free technique for fabricating submicron complex oxide structures has been developed based on selective epitaxial growth. The crystallinity and hence the conductivity of the complex oxide is inhibited by amorphous SrTiO₃ (STO). Using a combination of pulsed laser deposition and electron-beam lithography, amorphous STO barriers are first deposited on a single-crystal substrate. A thin film is then deposited on the patterned substrate with the amorphous STO barriers acting to electrically and physically isolate different regions of the film. Since no chemical or physical etchants come in contact with the deposited film, its integrity and stability are preserved. This technique has produced submicron YBa₂Cu₃O_{7- δ} and La_{2/3}Ca_{1/3}MnO₃ structures.

© 2005 American Institute of Physics. [DOI: 10.1063/1.1925781]

Fabrication of complex oxide nanostructures is important from both a physical and technological standpoint. Many complex oxides exhibit interesting electrical behavior including high- T_c superconductivity, colossal magnetoresistance (CMR), and ferroelectricity. Potential device applications including high sensitivity sensors,¹ flux flow transistors,² ferroelectric field effect transistors,³ and magnetic memory⁴ require suitable microfabrication techniques. However, due to inherent stoichiometric and structural complexities associated with complex oxides, producing high-quality submicron structures has proven difficult because conventional methods tend to require etching of the complex oxide.

In this letter, we present a technique for fabricating submicron complex oxide structures, which requires no chemical or physical etching. Based on selective epitaxial growth, a single-crystal substrate is patterned both vertically and laterally by the deposition of amorphous SrTiO₃ (STO) barriers. The amorphous nature of the STO barriers acts to ensure that any material deposited on top of the barriers is electrically insulating. This technique has the advantage that complex structures can be fabricated without any degradation due to chemical or physical etching. The minimum dimensions of the microstructure are well defined by the amorphous STO barriers and are not determined by diffusive processes. This technique also allows for the deposition of passivation layers which can improve the stability of the complex oxide.⁵

Conventional techniques for fabricating submicron complex oxide structures involve either postdeposition etching of the oxide or patterning of the substrate before deposition. Postdeposition patterning has commonly been obtained using wet-chemical etching of the oxide in solutions of bromine in ethanol,⁶ ethylenediaminetetraacetic acid,⁷ phosphoric acid,⁸ or hydrofluoric acid.⁹ However, wet-chemical etching of YBa₂Cu₃O_{7- δ} (YBCO) thin films has been shown to cause a significant increase in the high-frequency surface resistance as well as to cause insulating dead layers and a change in the surface morphology at the exposed surfaces.¹⁰ Physical etching methods, such as reactive ion etching,¹¹ focused ion beam etching,¹² and pulsed laser etching¹³ have also been

used to pattern complex oxide microstructures. However, these methods can cause physical damage to the exposed surfaces of the thin film. Also, heat generated from these physical processes can be sufficiently large to alter the doping and hence their electrical transport properties of the oxide.

Submicron structures can also be fabricated by patterning a single-crystal substrate prior to deposition. The substrate is patterned such that regions of the deposited film are physically separated through the creation of ridge or trench structures¹⁴ or electrically isolated through the inhibition of the conductivity of select regions. The inhibition of conductivity can be achieved by destroying the local crystallinity of select regions. This can be achieved by diffusion of Si,¹⁵ SiO₂,⁵ Si_xN_y,¹⁶ or Ti¹⁷ or by selectively determining where epitaxial growth can occur through the deposition of a Ti or W layer on selective regions of the substrate.¹⁸

Our chemical-free procedure for fabricating complex submicron structures is outlined schematically in Fig. 1. First, a poly(methylmethacrylate) (PMMA) mask is defined on a single crystal STO substrate by electron-beam lithography (EBL). A ≈ 700 nm layer of 7% PMMA in anisole with a molecular weight of 450 amu is spun onto a single-crystal STO substrate at 4500 rpm for 45 s. The resist is then baked on a hot plate at 180 °C for 5 min. The resist is then exposed by EBL using a JEOL IC-848A, tungsten filament scanning electron microscope at an accelerating voltage of 30 kV, probe current of 8 pA, and a line dosage of 0.9 nC/cm. The low probe current was used to allow sufficient time for any accumulated charge to dissipate, in order to reduce any electron charging effects that could readily occur when imaging an insulating material. The resist is then developed in a 3:1 solution of isopropyl alcohol (IPA) to methyl isobutyl ketone for 30 s and then rinsed in IPA.

After the mask has been defined, a layer of amorphous STO is then deposited by pulsed laser deposition (PLD) using a 248 nm KrF excimer laser at a laser energy density of ≈ 1.2 J/cm². The STO is pulsed laser ablated at an oxygen partial pressure of 20 mTorr and at ambient temperature to ensure no evaporation or diffusion of the PMMA mask occurs. An ablation time of 30 min using a pulsed laser repetition rate of 10 Hz results in the deposition of ≈ 350 nm of

^{a)}Electronic mail: patrick.morales@utoronto.ca

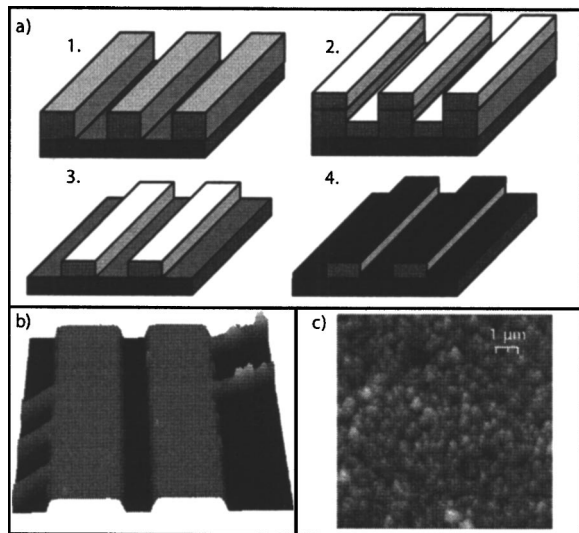


FIG. 1. (a) Selective epitaxial nanofabrication technique: (1) A PMMA mask is defined using EBL. (2) A layer of amorphous STO is deposited by PLD at ambient temperature. (3) The PMMA mask is removed leaving only the amorphous STO deposited directly on the substrate. (4) A complex oxide thin film is deposited on the patterned substrate. The material deposited on top of the amorphous STO barriers is of poor crystallinity and hence poor conductivity. (b) Three-dimensional AFM image of a typical patterned substrate showing the amorphous STO barriers. (c) AFM image of a 50 nm YBCO thin film deposited on the amorphous STO barrier, showing the amorphous nature of the deposited YBCO with an average (root-mean-square) surface roughness of 19 ± 2 nm.

amorphous STO. The remaining PMMA is then removed by acetone in an ultrasonic bath for 45 s, leaving behind an inhibitive pattern of amorphous STO. A complex oxide film, such as YBCO or $\text{La}_{2/3}\text{Ca}_{1/3}\text{MnO}_3$ (LCMO), can then be deposited by PLD using typical ablation conditions. Since the deposition of the complex oxide is the last step in the process, the integrity of the resulting structure is preserved, as it does not undergo subsequent heating due to physical bombardment or come in contact with chemical etchants.

The electrical transport properties of our fabricated microstructures were characterized by standard four-point phase sensitive ac resistance versus temperature measurements, as well as synchronous pulsed current versus voltage (I - V) and voltage versus current (V - I) measurements. In the latter technique, pulses of 200 μs with a duty cycle of 5% were used in order to minimize any effects of Joule heating.

Submicron YBCO strips fabricated using our technique exhibit superconducting critical temperatures, T_c , of 80–92 K, with transition widths of 1–10 K. YBCO strips show room-temperature resistivities of tens to several hundreds of $\mu\Omega$ cm and critical current densities, j_c , on the order of 10^7 A/cm², which approach those of unpatterned YBCO thin films. To ensure that an applied current was indeed confined to the selective regions of the film, we also measured the YBCO film that was deposited on the amorphous STO barriers. These control samples show no superconducting transition and exhibit room-temperature resistivities on the order of 10^6 $\mu\Omega$ cm. An atomic force micrograph (AFM) shown in Fig. 1 confirms the amorphous nature of the deposited YBCO.

Previous transport studies on chemically patterned cuprate samples ranging from 100 nm to 2 μm in width have been reported. Highly nonlinear I - V characteristics and anomalous resistance versus temperature behavior have been

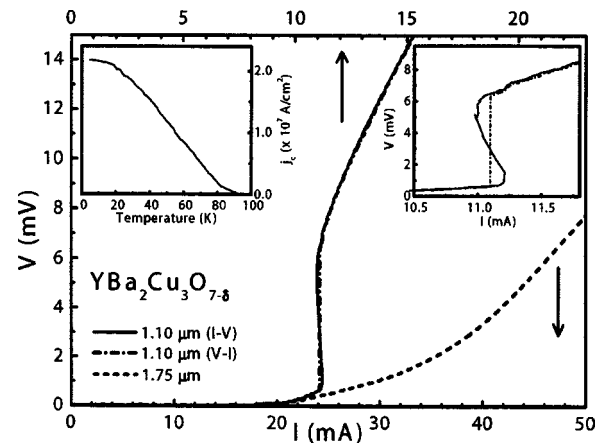


FIG. 2. I - V characteristics of YBCO microstrips of differing widths at 24 K. The V - I of the narrower (1.10 μm) microstrip exhibits a characteristic step. The I - V measurement of the strip shows that this step coincides with an s -shaped conductance region (inset upper right) both of which are consistent with phase-slip behavior. A V - I measurement of a wider YBCO strip does not exhibit such characteristic behavior. Upper left inset shows the critical current density versus temperature of the 1.10 μm YBCO strip.

attributed to either collective flux flow, phase slips, or mesoscopic domains.^{19–23} The V - I characteristics of YBCO microstrips fabricated using our technique are shown in Fig. 2. For wider strips, the V - I characteristic can be described by a power-law relationship caused by thermally activated flux creep and flux flow. However, as the applied current becomes more confined in a narrower strip, the power-law relation is only valid below some threshold value of applied current. At this threshold value, a discontinuity in the voltage occurs and the V - I relationship becomes linear. An I - V measurement of the same microstrip shows that voltage discontinuity coincides with an s -shaped negative conductance region (see inset Fig. 2). Both the discontinuity of the voltage in the V - I characteristic and the s -shaped I - V characteristic of the microstrip are consistent with phase-slip behavior due to the lateral confinement of the superconductor.^{24,25} An investigation of the phase-slip behavior in our YBCO microstrips as well as information derived from such behavior on the dynamics of the superconducting order parameter is the focus of separate papers.^{26,27}

Submicron LCMO strips were also fabricated using our technique. Submicron LCMO strips are of interest because their magnetoresistive properties can be tuned by externally applied strain.²⁸ Resistance versus temperature measurements of strips of differing widths at zero field are shown in Fig. 3. Fabricated submicron LCMO strips show a maximum in resistance, T_m , ranging from 220 K to 300 K. The position of T_m has been shown to be highly dependent on stress relaxation and improved crystallinity resulting from grain growth.²⁹ A field dependent study of the CMR properties of submicron LCMO strips fabricated using our technique will be presented in a separate paper.³⁰

In summary, we have developed a chemical-free technique for fabricating submicron complex oxide structures. The technique is based on selective epitaxial growth of a complex oxide thin film. The crystallinity and hence the conductivity of the complex oxide thin film are inhibited by amorphous SrTiO_3 barriers deposited upon a single-crystal substrate. This technique has been applied to fabricate strips of submicron high- T_c superconducting YBCO and CMR LCMO.

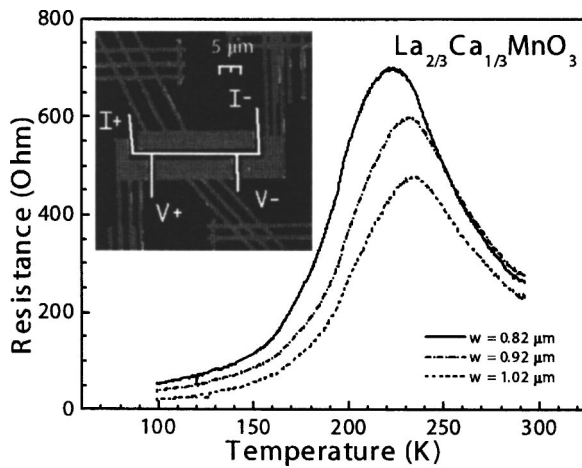


FIG. 3. Resistance versus temperature measurements for LCMO microstrips of differing widths. Inset shows an AFM image of a typical microstrip with an overlay indicating the current and voltage leads.

The authors acknowledge assistance by Stephanie Chiu and Eugenia Tam and funding from: NSERC, CFI/OIT, MMO/EMK, and the Canadian Institute for Advanced Research under the Quantum Materials Program.

¹A. I. Braginski, IEEE Trans. Appl. Supercond. **9**, 2825 (1999).

²J. S. Martens, D. S. Ginley, J. B. Beyer, J. E. Nordman, J. E. Honenwarter, and G. K. G. Honenwarter, IEEE Trans. Appl. Supercond. **1**, 95 (1991).

³R. Ramesh, A. Inam, W. K. Chan, B. Wilkens, K. Myers, K. Remschmig, D. L. Hart, and J. M. Tarascon, Science **252**, 944 (1991).

⁴A. M. Grishin, S. I. Khartsev, and P. Johnsson, Appl. Phys. Lett. **74**, 1015 (1999).

⁵C. A. Copetti, U. Gassig, W. Zander, J. Schubert, and C. Buchal, Appl. Phys. Lett. **61**, 3041 (1992); R. A. Barnes and R. A. Laudise, *ibid.* **51**, 1373 (1987).

⁶R. P. Vasquez, B. D. Hunt, and M. C. Foote, Appl. Phys. Lett. **53**, 2692 (1988).

⁷F. K. Shokoohi, L. M. Schiavone, C. T. Rogers, A. Inam, X. D. Wu, L. Nazar, and T. Venkatesan, Appl. Phys. Lett. **55**, 2661 (1990); J. A. Beall, M. W. Cromar, T. E. Harvey, M. E. Johansson, R. H. Ono, C. D. Reintsema, D. A. Rudman, S. E. Asher, A. J. Nelson, and A. B. Swartzlander, IEEE Trans. Magn. **27**, 1596 (1991); C. I. H. Ashby, J. Martens, T. A. Plut, D. S. Ginley, and J. M. Phillips, Appl. Phys. Lett. **60**, 2147 (1992).

⁸W. G. Lyons, R. R. Bonetti, A. E. Williams, P. M. Mankiewich, M. L. O'Malley, J. M. Hamm, A. C. Anderson, R. S. Withers, A. Meulenberg,

and R. E. Howard, IEEE Trans. Magn. **27**, 2537 (1991).

⁹W. Eidelloth, W. J. Gallagher, R. P. Robertazzi, R. H. Koch, B. Oh, and R. L. Sandstrom, Appl. Phys. Lett. **59**, 1257 (1991).

¹⁰A. Roshko, S. E. Russek, K. A. Trott, S. C. Sanders, M. E. Johansson, J. S. Martens, and D. Zhang, IEEE Trans. Appl. Supercond. **5**, 1733 (1995).

¹¹S. Matsui, N. Takado, H. Tsuge, and K. Asakawa, Appl. Phys. Lett. **52**, 69 (1988); J. W. C. de Vries, B. Dam, M. G. J. Heijman, G. M. Stollman, M. A. M. Gijs, C. W. Hagen, and R. P. Griessen, *ibid.* **52**, 1904 (1988); P. Larsson, B. Nilsson, and Z. G. Ivanov, J. Vac. Sci. Technol. B **18**, 25 (2000).

¹²S. Matsui, Y. Ochiai, Y. Kojima, H. Tsuge, N. Takado, K. Askawa, H. Matsutera, J. Fujita, T. Yoshitake, and Y. Kubo, J. Vac. Sci. Technol. B **6**, 900 (1988); S. J. Kim and T. Yamashita, J. Appl. Phys. **89**, 7675 (2001).

¹³A. Inam, X. D. Wu, T. Venkatesan, S. B. Ogale, C. C. Chang, and D. Dijkkamp, Appl. Phys. Lett. **51**, 1112 (1987).

¹⁴P. Mohanty, J. Y. T. Wei, V. Ananth, P. Morales, and W. Skocpol, Physica C **408**, 666 (2004).

¹⁵Q. Y. Ma, E. S. Yang, G. V. Trayz, and C. A. Chang, Appl. Phys. Lett. **55**, 896 (1989).

¹⁶D. P. Kern, K. Y. Lee, R. B. Laibowitz, and A. Gupta, J. Vac. Sci. Technol. B **9**, 2875 (1991).

¹⁷C. Rossel, U. Kaufmann, H. Downar, and R. Schulz, Physica C **185**, 2551 (1991).

¹⁸C. A. J. Damen, H.-J. H. Smilde, D. H. A. Blank, and H. Rogalla, Supercond. Sci. Technol. **11**, 437 (1998).

¹⁹M. J. M. E. de Nivelles, G. J. Gerritsma, and H. Rogalla, Phys. Rev. Lett. **70**, 1525 (1993).

²⁰V. M. Dmitriev, I. V. Zolocheskii, and E. V. Kristenko, Physica C **235**, 1973 (1994).

²¹F. S. Jelila, J.-P. Maneval, F.-R. Ladan, F. Chibane, A. Marie-de-Ficquelmont, L. Méchin, J.-C. Villégier, M. Aprili, and J. Lesueur, Phys. Rev. Lett. **81**, 9 (1998).

²²M. M. Abdelhadi and J. A. Jung, Phys. Rev. B **67**, 054502 (2003).

²³J. A. Bonetti, D. S. Caplan, D. J. Van Harlingen, and M. B. Weissman, Phys. Rev. Lett. **93**, 087002 (2004); J. A. Bonetti, D. J. Van Harlingen, and M. B. Weissman, Physica C **388**, 343 (2003).

²⁴W. J. Skocpol, M. R. Beasley, and M. Tinkham, J. Low Temp. Phys. **16**, 145 (1974).

²⁵D. Y. Vodolazov, F. M. Peeters, L. Piraux, S. Matefi-Tempfli, and S. Michotte, Phys. Rev. Lett. **91**, 15 (2003).

²⁶P. Morales, M. DiCiano, and J. Y. T. Wei (unpublished).

²⁷P. Morales and J. Y. T. Wei (unpublished).

²⁸T. Y. Koo, S. H. Park, K.-B. Lee, and Y. H. Jeong, Appl. Phys. Lett. **71**, 977 (1997).

²⁹K. A. Thomas, P. S. I. P. N. de Silva, L. F. Cohen, A. Hossain, M. Rajeswari, T. Venkatesan, R. Hiskes, and J. L. MacManus-Driscoll, J. Appl. Phys. **84**, 3939 (1998).

³⁰P. Morales and J. Y. T. Wei (unpublished).